Compel

Coupled mechanical-electrostatic FE-BE analysis with FMM acceleration: application to a shunt capacitive MEMS switch

R.V. Sabariego
Department of Electrical Engineering and Computer Science (ELAP), University of Liège, Liège, Belgium
J. Gyselinck
Department of Electrical Engineering and Computer Science (ELAP), University of Liège, Liège, Belgium
P. Dular
Department of Electrical Engineering and Computer Science (ELAP), University of Liège, Liège, Belgium
J. De Coster
Department of Electrical Engineering (ESAT-MICAS), Katholieke Universiteit Leuven, Leuven, Belgium
F. Henrotte
Department of Electrical Engineering (ESAT-ELECTA), Katholieke Universiteit Leuven, Leuven, Belgium
K. Hameyer
Department of Electrical Engineering (ESAT-ELECTA), Katholieke Universiteit Leuven, Leuven, Belgium

COMPEL, Vol. 23 No. 4, 2004,
 ISSN 0332-1649

Coupled mechanical-electrostatic FE-BE analysis with FMM acceleration

Application to a shunt capacitive MEMS switch

R.V. Sabariego, J. Gyselinck and P. Dular
Department of Electrical Engineering and Computer Science (ELAP), University of Liège, Liège, Belgium

J. De Coster
Department of Electrical Engineering (ESAT-MICAS), Katholieke Universiteit Leuven, Leuven, Belgium

F. Henrotte and K. Hameyer
Department of Electrical Engineering (ESAT-ELECTA), Katholieke Universiteit Leuven, Leuven, Belgium

Keywords *Finite element analysis, Boundary-elements methods*

Abstract *This paper deals with the coupled mechanical-electrostatic analysis of a shunt capacitive MEMS switch. The mechanical and electrostatic parts of the problem are modelled by the FE and BE methods, respectively. The fast multipole method is applied to reduce the storage requirements and the computational cost of the BE electrostatic model. An adaptive truncation expansion of the 3D Laplace Green function is employed. The strong interaction between the mechanical and electrostatic systems is considered iteratively.*

1. Introduction

Electrostatic parallel-plate actuators are widely used in many types of microelectromechanical systems (MEMS). MEMS switches can be used in series or shunt mode and their contacts can be resistive or capacitive (Brown, 1998; Tilmans, 2002). A shunt capacitive MEMS switch consists of a metal armature (bridge) suspended over a bottom conductor, e.g. the center conductor of a coplanar waveguide, mechanically anchored and electrically connected to the ground. A thin dielectric film is deposited on the bottom conductor (Figure 1). When the bridge is up, the capacitance of the switch is very small and the RF signal passes through freely (the RF switch is on). By applying a bias voltage the switch is actuated: an electrostatic force occurs between the top and bottom conductors and the bridge is pulled down, the capacitance increases and causes an RF short to ground (the RF switch is off) (Brown, 1998; Tilmans, 2002).

These actuators can be treated, in first approximation, as lumped spring-mass systems with a single mechanical degree of freedom (Tilmans, 2002). This analysis is

The research was carried out in the frame of the Inter-University Attraction Poles IAP P5/34 for fundamental research funded by the Belgian government. P. Dular is a Research Associate with the Belgian National Fund for Scientific Research (FNRS.).

COMPEL: The International Journal for Computation and Mathematics in Electrical and Electronic Engineering
Vol. 23 No. 4, 2004
pp. 876-884

0332-1649
DOI 10.1108/03321640410553300

helpful for physical insight, but disregards important effects such as the bending of the top plate and the stiction between the bridge and the bottom contact (Brown, 1998). The performance of RF MEMS switches strongly depends on the deformation of the top electrode. A detailed knowledge of the exact deformation for an accurate estimate of the capacitance is thus crucial.

A boundary element (BE) approach is particularly suited for the analysis of the real electrostatic problem (Farina and Rozzi, 2001). Indeed, the BE method provides a rigorous treatment for open problems and allows to consider the deformation without any remeshing. The elastic deformation of the top plate (and the suspension beams) can be handled by means of a finite element (FE) model. It depends directly on the electrostatic force exerted on the bridge and the material properties. The electrostatic field induces a force distribution, the value of which increases when the distance between the top and bottom plate diminishes. This interaction between the electrostatic and mechanical systems can be considered iteratively.

A significant disadvantage of the BE electrostatic model is that it leads to a fully populated system matrix limiting the size of the problems to be handled. The fast multipole method (FMM) (Rokhlin, 1983), combined with an iterative solver, e.g. GMRES (Saad and Schultz, 1986), can be employed to overcome this limitation by diminishing both storage requirements and the computational time. The FMM method has succesfully been applied to solve electrostatic problems in Buchau *et al.*, 2000; and Nabors and White, 1991.

In this paper, we discuss the coupled mechanical-electrostratic analysis of a capacitive MEMS shunt switch. Section 2 outlines the electrostatic BE model of the actuator. The FMM is briefly described in Section 3. An adaptive truncation scheme for the 3D Laplace Green function is employed. Section 4 deals with the elastic deformation FE model. In Section 5, the application example is considered. Simulated results obtained by means of different software packages are briefly compared.

2. Electrostatic BE model

We consider an electrostatic problem in $\mathbb{R}^3$. The conductors are embedded in multiple homogeneous isotropic dielectrics and set to fixed potentials.

The surfaces of conductors and dielectrics $\Gamma = \Gamma_C \cup \Gamma_D$ are discretised with plane triangles. The surface charge density q is assumed to be piecewise constant. The conductors can be replaced by their charge density on their surfaces q_c and

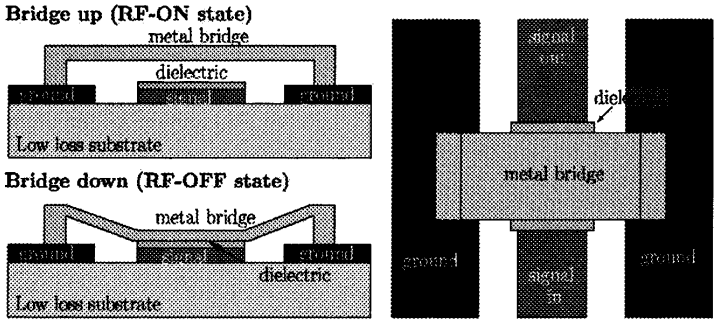

Figure 1.
Electrostatically actuated capacitive shunt switch implemented on a CPW transmission line. Side and top views

the homogeneous dielectrics by the polarisation charge q_p. The total charge on the interface conductor-dielectric Γ_C is given by the sum of both types of charges. Analogously, on the surface between two dielectrics Γ_D the total charge is the sum of the polarisation charge due to both dielectrics (Rao *et al.*, 1984). The following system of n_q linear equations has to be solved

$$\mathbf{MQ} = \mathbf{B}, \tag{1}$$

where $\mathbf{Q} = [q_1 \ldots q_{n_q}]^T$ contains the charge densities on the elements and $\mathbf{B} = [b_1 \ldots b_{n_q}]^T$ depends on the boundary conditions. For an element on the surface of a conductor Γ_C, the entry in $\mathbf{B}$ is the imposed potential; for an element on the interface between two dielectrics Γ_D, the entry in $\mathbf{B}$ is zero. The elements of the dense nonsymmetric matrix $\mathbf{M}$ when k is an element on a conductor are given by

$$M_{k,l} = \frac{1}{\varepsilon_0} \oint_{\Gamma_l} G(\rho_k)\, d\Gamma' \quad \text{with} \quad G(\rho_k) = \frac{1}{4\pi\rho_k}. \tag{2}$$

$G(\rho_k)$ is the 3D Laplace Green function, $\rho_k = |\underline{r}_k - \underline{r}'|$ being the distance between a source point $\underline{r}'$ (on $\Gamma_l \in \Gamma$) and an observation point $\underline{r}_k$ (on Γ_C). Considering the continuity of the normal component of the dielectric displacement $\underline{d} = \varepsilon\underline{e}$ at the dielectric-to-dielectric interface, Γ_D, the elements of $\mathbf{M}$ if k is an element on Γ_D read:

$$M_{k,l} = \begin{cases} \dfrac{\varepsilon_{k2} - \varepsilon_{k1}}{\varepsilon_0(\varepsilon_{k1} + \varepsilon_{k2})} \displaystyle\oint_{\Gamma_l} \operatorname{grad} G(\rho_k) \cdot \underline{n}_k \, d\Gamma', & k \neq l, \\ \dfrac{1}{2\varepsilon_0}, & k = 1. \end{cases} \tag{3}$$

where $\underline{n}_k$ is the outward-normal unit vector pointing into the dielectric with permittivity ε_{k2}. The integrals in equations (2) and (3) can be evaluated analytically (Graglia, 1993).

The electrostatic force $\underline{F}_e$ distribution can be calculated as

$$\underline{F}_e(\underline{r}) = \frac{1}{2} q(\underline{r}) \underline{e}(\underline{r}). \tag{4}$$

The electric field $\underline{e}$ as $\underline{r}$ approaches the interface conductor-dielectric can be expressed as (Rao *et al.*, 1984):

$$\underline{e}^{\pm}(\underline{r}) = \pm \underline{n} \frac{q(\underline{r})}{2\varepsilon_0} + \frac{1}{4\pi\varepsilon_0} \langle \operatorname{grad} G(\rho), q(\underline{r}') \rangle_\Gamma, \tag{5}$$

where + indicates the outer face of the conducting surface and − the inner one, $\underline{n}$ is the normal unit vector pointing outside the conductor and $\langle \cdot, \cdot \rangle_\Gamma$ denotes a surface integral on Γ of the product of its arguments. As inside the conductor $\underline{e}^- = 0$, considering equation (5), it follows that $\underline{e}^+$ on the surface of the conductor is given by

$$\underline{e}^+(\underline{r}) = \underline{n} \frac{q(\underline{r})}{\varepsilon_0}. \tag{6}$$

Substituting equation (6) in equation (4), the expression of $\underline{F}_e$ as a function of the charge distribution is obtained as

$$\underline{F}_e(\underline{r}) = \frac{1}{2\varepsilon_0} q^2(\underline{r})\underline{n}. \tag{7}$$

3. Fast multipole method

The implementation of the FMM requires the grouping of the elements on the surface boundary

$$\Gamma = \cup_{g=1}^{\#g} \Gamma_g.$$

A good choice is a scheme based on cubes, i.e. un octree (Buchau *et al.*, 2000; Nabors and White, 1991). Note that in a single level FMM, as described in the present paper, only the finest level of the octree is. The interactions between the distant groups are then determined by means of the multipole expansion of the Laplace Green function.

3.1 Multipole expansion

Let Γ_s be a source group with center $\underline{r}_{sc}$ and a source point $\underline{r}_s$, and Γ_o an observation group with center $\underline{r}_{oc}$ and an observation point $\underline{r}_o$. We define the vectors $\underline{r} = \underline{r}_o - \underline{r}_{oc} = (r, \theta, \phi)$, $\underline{r}_c = \underline{r}_{oc} - \underline{r}_{sc} = (r_c, \theta_c, \phi_c)$ and $\underline{r}' = \underline{r}_{sc} - \underline{r}_s = (r', \theta', \phi')$. Omitting the factor $1/4\pi$, the 3D Laplace Green function (2), with $\rho = |\underline{r}_o - \underline{r}_s|$, is expanded as (Rokhlin, 1983):

$$\frac{1}{\rho} = \Re\left(\sum_{m=0}^{\infty}\sum_{n=-m}^{m}\sum_{u=0}^{\infty}\sum_{v=-u}^{u} \mathscr{D}_{m,n}\,\mathscr{T}_{m+u,n+v}\,\mathscr{A}_{u,v}\right), \tag{8}$$

with

$$\mathscr{D}_{m,n}(\underline{r}) = \frac{r^m \mathscr{L}_m^n(\theta, -\phi)}{(m+n)!}, \tag{9}$$

$$\mathscr{T}_{m+u,n+v}(\underline{r}_c) = \frac{(m+u-(n+v))!}{r_c^{m+u+1}} \mathscr{L}_{m+u}^{n+v}(\theta_c, \phi_c), \tag{10}$$

$$\mathscr{A}_{u,v}(\underline{r}') = \frac{r'^u \mathscr{L}_u^v(\theta', -\phi')}{(u+v)!}, \tag{11}$$

where $\mathscr{L}_m^n(\theta, \phi) = P_m^n(\cos\theta)e^{in\phi}$, P_m^n being the Legendre function of degree m and order n. The imaginary number is denoted i and $\Re$ indicates the real part.

In practice, the multipole expansion (8) must be truncated by taking $0 \le m \le p$ and $0 \le u \le p$, where the truncation number p must be sufficiently large to limit the error to a prescribed value ε. In most cases, the conventional choice $p = \log_2(1/\varepsilon)$ (Rokhlin, 1983) is too conservative. Indeed, if $r' \ll r_c$ and $r \ll r_c$, a smaller number of terms suffices. Let us consider the radii of the source and observation groups, $R_s = \max_{\Gamma_s}(r')$, $R_o = \max_{\Gamma_o}(r)$, and the distance between their centers d. A more economic law $p = p(R_s/d, R_o/d, \varepsilon)$, proposed by some of the authors in Sabariego *et al.* (2004), considers those distances.

The function grad G in equation (3) can be expanded in a similar way. It suffices to derive equation (9) with respect to the coordinates of the observation point.

$$\underline{F}_e(\underline{r}) = \frac{1}{2\varepsilon_0} q^2(\underline{r})\underline{n}. \tag{7}$$

3. Fast multipole method

The implementation of the FMM requires the grouping of the elements on the surface boundary

$$\Gamma = \cup_{g=1}^{\#g} \Gamma_g.$$

A good choice is a scheme based on cubes, i.e. un octree (Buchau *et al.*, 2000; Nabors and White, 1991). Note that in a single level FMM, as described in the present paper, only the finest level of the octree is. The interactions between the distant groups are then determined by means of the multipole expansion of the Laplace Green function.

3.1 Multipole expansion

Let Γ_s be a source group with center $\underline{r}_{sc}$ and a source point $\underline{r}_s$, and Γ_o an observation group with center $\underline{r}_{oc}$ and an observation point $\underline{r}_o$. We define the vectors $\underline{r} = \underline{r}_o - \underline{r}_{oc} = (r, \theta, \phi)$, $\underline{r}_c = \underline{r}_{oc} - \underline{r}_{sc} = (r_c, \theta_c, \phi_c)$ and $\underline{r}' = \underline{r}_{sc} - \underline{r}_s = (r', \theta', \phi')$. Omitting the factor $1/4\pi$, the 3D Laplace Green function (2), with $\rho = |\underline{r}_o - \underline{r}_s|$, is expanded as (Rokhlin, 1983):

$$\frac{1}{\rho} = \Re\left(\sum_{m=0}^{\infty}\sum_{n=-m}^{m}\sum_{u=0}^{\infty}\sum_{v=-u}^{u} \mathscr{D}_{m,n}\,\mathscr{T}_{m+u,n+v}\,\mathscr{A}_{u,v}\right), \tag{8}$$

with

$$\mathscr{D}_{m,n}(\underline{r}) = \frac{r^m \mathscr{L}_m^n(\theta, -\phi)}{(m+n)!}, \tag{9}$$

$$\mathscr{T}_{m+u,n+v}(\underline{r}_c) = \frac{(m+u-(n+v))!}{r_c^{m+u+1}} \mathscr{L}_{m+u}^{n+v}(\theta_c, \phi_c), \tag{10}$$

$$\mathscr{A}_{u,v}(\underline{r}') = \frac{r'^u \mathscr{L}_u^v(\theta', -\phi')}{(u+v)!}, \tag{11}$$

where $\mathscr{L}_m^n(\theta, \phi) = P_m^n(\cos\theta)e^{in\phi}$, P_m^n being the Legendre function of degree m and order n. The imaginary number is denoted i and $\Re$ indicates the real part.

In practice, the multipole expansion (8) must be truncated by taking $0 \le m \le p$ and $0 \le u \le p$, where the truncation number p must be sufficiently large to limit the error to a prescribed value ε. In most cases, the conventional choice $p = \log_2(1/\varepsilon)$ (Rokhlin, 1983) is too conservative. Indeed, if $r' \ll r_c$ and $r \ll r_c$, a smaller number of terms suffices. Let us consider the radii of the source and observation groups, $R_s = \max_{\Gamma_s}(r')$, $R_o = \max_{\Gamma_o}(r)$, and the distance between their centers d. A more economic law $p = p(R_s/d, R_o/d, \varepsilon)$, proposed by some of the authors in Sabariego *et al.* (2004), considers those distances.

The function grad G in equation (3) can be expanded in a similar way. It suffices to derive equation (9) with respect to the coordinates of the observation point.

3.2 Application to the BE model

Two groups Γ_s and Γ_o are said to be "far" groups if $R_s/d < \tau$ and $R_o/d < \tau$, where d is the distance between the group centers and τ is chosen smaller than 1/2.

For demonstrating the FMM, the BE dense matrix $\mathbf{M}$ equations (2) and (3) can be formally written as

$$\mathbf{M} \approx \mathbf{M}^{\text{near}} + \mathbf{M}^{\text{far}} = \mathbf{M}^{\text{near}} + \underbrace{\sum_{o=1}^{\#g} \sum_{s=1}^{\#g} \mathbf{M}_{o,s}^{\text{far}}}_{\Gamma_o, \Gamma_s \text{far}}. \tag{12}$$

Let us consider the degrees of freedom q_k and q_l of q in the respective far groups $\Gamma_o \in \Gamma_C$ and $\Gamma_s \in \Gamma$. Substituting equation (8) in equation (2), the contribution to the corresponding element $(M_{o,s}^{\text{far}})_{k,l}$ in M^{far} is given by

$$\Re\left(\sum_{m=0}^{p} \sum_{n=-m}^{m} M_{o,k,m,n}^{\mathscr{D}} \sum_{u=0}^{p} \sum_{v=-u}^{u} M_{m+u,n+v}^{\mathscr{T}} M_{s,l,u,v}^{\mathscr{A}}\right), \tag{13}$$

$$M_{o,k,m,n}^{\mathscr{D}} = \int_{\Gamma_{o,k}} \mathscr{D}_{m,n} \, \mathrm{d}\Gamma, \qquad M_{s,l,u,v}^{\mathscr{A}} = \int_{\Gamma_{s,l}} \mathscr{A}_{u,v} \, \mathrm{d}\Gamma, \tag{14}$$

$$M_{m+u,n+v}^{\mathscr{T}} = \frac{1}{4\pi\varepsilon_0} \mathscr{T}_{m+u,n+v}. \tag{15}$$

The iterative solution of the system of algebraic equations requires the multiplication of $\mathbf{M}^{\text{far}}$ by a trial vector $\mathbf{Q}$. Group by group, the field produced by the electric charge q in the considered group is aggregated into its center by equation (14). This aggregated field is then subsequently translated to the centers of all the far groups by equation (15), and finally, the aggregated and translated field are disaggregated into the degrees of freedom of the far groups, thanks to equation (14).

The multiplication of $\mathbf{M}^{\text{far}}\mathbf{Q}$ is further accelerated by means of the adaptive truncation scheme following the law $p = p(R_s/d, R_o/d, \varepsilon)$ (Sabariego *et al.*, 2004). In case of preconditioning of the iterative solver, the preconditioner is based on the sparse matrix comprising the BE near-field interactions.

The assembly stage of the FMM consists in calculating and storing the required complex numbers $M_{o,k,m,n}^{\mathscr{D}}$, $M_{m+u,n+v}^{\mathscr{T}}$ and $M_{s,l,u,v}^{\mathscr{A}}$. The matrix $\mathbf{M}^{\text{far}}$ itself is never built. The integrations in equation (14) are done numerically, but as we are dealing with far interactions a limited number of Gauss integration point suffices. The matrix $\mathbf{M}^{\text{near}}$ is calculated in the conventional way (see previous Section) and stored using a sparse storage scheme. For the $\mathbf{M}^{\mathscr{D}}$ and $\mathbf{M}^{\mathscr{A}}$ data of a given group, the truncation number p considered during the FMM assembly stage is determined by its closest far group, $p = p_{\max}$. For the $\mathbf{M}^{\mathscr{T}}$ data, the truncation number p is determined by the two groups Γ_s and Γ_o involved in the translation, $p = p_{\text{so}}$. During the iterative process, the aggregation step is carried out with $p = p_{\max}$, while $p = p_{\text{so}}$ suffices for the translation and disaggregation.

4. Elastic deformation-FE model

The upper electrode is deformed by the electrostatic force exerted on it. The elastic equation has to be considered alongside the electrostatic equations. For linear elastic isotropic materials, it reads:

$$\mathbf{D}^{\mathrm{T}}\underline{\underline{E}}\mathbf{D}\underline{u} + \underline{F} = 0, \tag{16}$$

where $\mathbf{D}$ is the differential operator matrix with transpose $\mathbf{D}^{\mathrm{T}}$, $\underline{\underline{E}}$ is the elasticity tensor, $\underline{u}$ is the displacement vector and $\underline{F}$ is the total force exerted. The elasticity tensor $\underline{\underline{E}}$ relates the stress tensor with the strain tensor. It depends on the Young's modulus E and the Poisson's ratio ν (Pilkey, 2002).

5. Application example

The shunt capacitive MEMS switch shown in Figure 2 is chosen as the test case. It concerns a perforated top plate (thickness = 4 μm) suspended by a set of beams, and a bottom plate (thickness = 0.5 μm) coated with a thin dielectric layer (thickness = 0.2 μm, $\varepsilon_r = 7$). The beam suspension allows a vertical movement with respect to the fixed bottom plate. The top plate is perforated to facilitate the under-etching of the structure. The dimension of the holes is 25 μm × 25 μm, with a pitch of 50 μm. The mechanical material constants of the top plate are $E = 70$ Gpa and $\nu = 0.3$.

The BE method with FMM acceleration is applied for solving the electrostatic problem while the mechanical problem is handled by a FE model. All the above mentioned methods are implemented in GetDP (2003). The behaviour of the switch is simulated using a discretisation consisting of 6,544 triangles and 11,151 tetrahedra, which yields 6,544 degrees of freedom for the piecewise element constant charge q and 56,331 degrees of freedom for the second-order interpolation of the displacement $\underline{\mu}$.

The optimal number of FMM groups (for this particular mesh) is found to be 35. The maximum and average truncation number are $p_{\max} = 6$ and $p_{\mathrm{av}} = 4$ for $R_{\mathrm{far}} = 135$ μm and $\varepsilon = 10^{-6}$.

The electrostatic and mechanical systems are solved iteratively by obtaining the new electrostatic force distribution and the new displacement. The number of

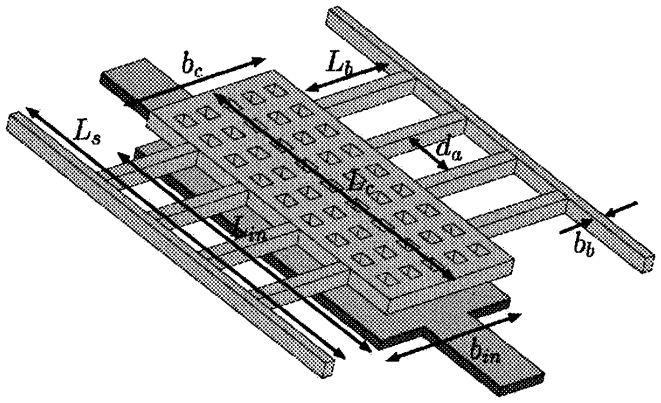

Figure 2.
Geometry of shunt capacitive MEMS switch: $L_c = 475$ μm, $b_c = 275$ μm, $L_{in} = 485$ μm, $b_{in} = 285$ μm, $L_s = 625$ μm, $L_b = 205$ μm, $b_b = 20$ μm, and $d_a = 80$ μm

iterations required for sufficient convergence of, e.g. the capacitance increases as the applied bias voltage approaches the pull-in voltage and the deformation of the top plate becomes bigger.

The calculated zero-voltage capacitance $C_{V=0}$ and pull-in voltage V_{IN} are 0.36 pF 14.2 V, respectively.

The deformation of the top electrode for a bias voltage of 11 V for the successive iterations is shown in Figure 3. Convergence is achieved after nine iterations.

The results obtained with GetDP (GetDP, 2003) are compared with those given by the commercial software packages Coventor (Coventor, Inc. 2003) and FemLab (FemLab, 1997-2004). In the simulations performed with the commercial programs, only a quarter of the geometry is considered. In the Coventor simulation, the electrostatic part is modelled by means of the BE method while the mechanical part is dealt with using the FE method and second-order elements. Only symmetry boundary conditions are considered for the mechanical problem. In the FemLab computation, the whole electromechanical problem is solved by the FE method. Symmetry conditions are imposed for the electrostatic problem. With regard to the mechanical part, the elastic behaviour of the suspension (beams) is approximated by a stiffness constant (Brown, 1998; Tilmans, 2002). For the face of the top electrode that is coupled with the suspension, the displacement is obtained by dividing the total electrostatic force by the stiffness constant.

The nominal capacitance $C_{V=0}$ obtained by Coventor and Femlab is 0.4 and 0.37 pF, respectively. The pull-in calculated voltage is 14.24 V for Coventor and 17.25 V.

The computed value of the capacitance as a function of the applied voltage is shown in Figure 4 for the three different solvers. The curves $C - V$ obtained with GetDP and FemLab agree well for low applied voltage, when the deformation is small. As the applied voltage increases, an accurate estimate of the displacement becomes critical, the approximation used for the suspension does not suffice. On the contrary, the agreement between the curves obtained with GetDP and Coventor is better as the voltage increases. The influence of three quarters of the device are disregarded for the electrostatic computation, but the mechanical part is solved accurately. Figure 5 shows

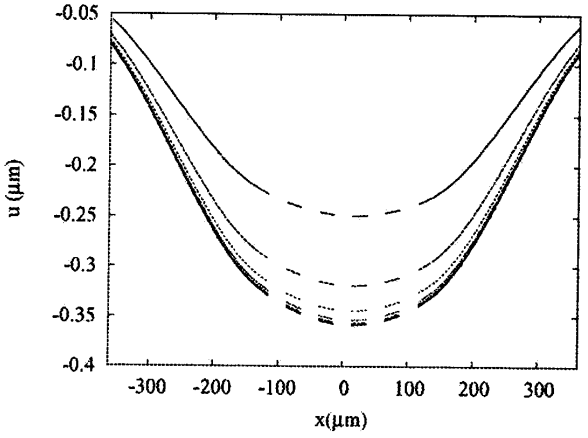

Figure 3.
Convergence of the vertical displacement along a line through the suspension beams and perforated plate for an applied bias voltage of 11 V

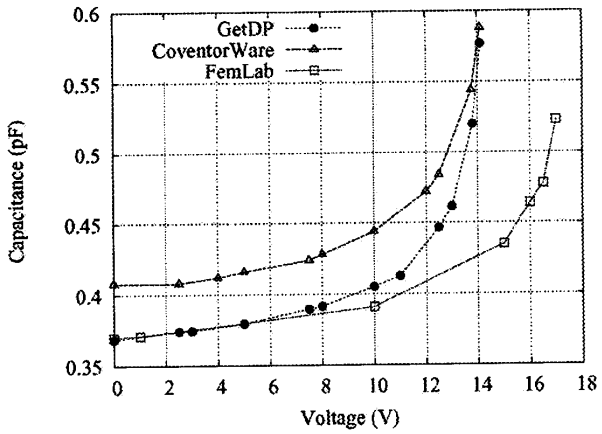

Figure 4.
Calculated capacitance vs the applied bias voltage simulation explains the divergence of the curves

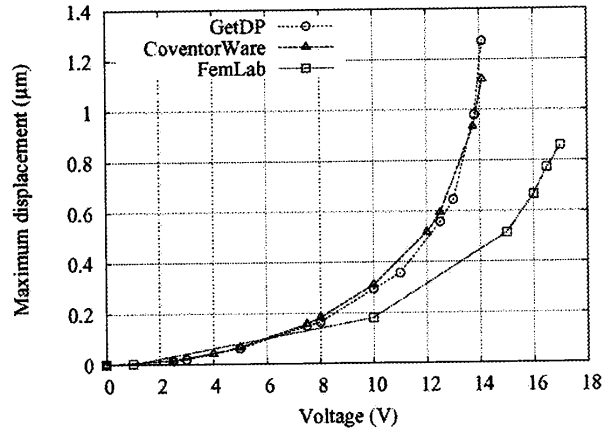

Figure 5.
Maximum vertical displacement of the top electrode vs the applied bias voltage

the maximum vertical displacement of the top electrode as a function of the applied bias voltage. A good agreement between the values obtained by means of GetDP and Coventor is observed. Approximation is used for the mechanical problem with a stiffness constant for modelling the suspension in the FemLab.

6. Conclusion

A shunt capacitive MEMS switch has been modelled. The BE method, accelerated by the FMM, and the FE method have been applied to solve the electrostatic and mechanical problem, respectively. An adaptive truncation scheme for the 3D Laplace Green function has been employed. The results have been compared with those obtained with the commercial packages Coventor and FemLab.

References

Brown, E.R. (1998), "RF-MEMS switches for reconfigurable integrated circuits", *IEEE Trans. on Microwave Theory and Techniques*, Vol. 46 No. 11, pp. 1868-80.

Buchau, A., Huber, C.J., Rieger, W. and Rucker, W.M. (2000), "Fast BEM computations with the adaptive multilevel fast multipole method", *IEEE Transactions on Magnetics*, Vol. 36 No. 4, pp. 680-4.

Coventor, Inc. (2003), *Accelerating MEMS Innovations*, 4001 Weston Parkway, Cary, NC 27513, available at: www.coventor.com, USA

Farina, M. and Rozzi, T. (2001), "A 3D integral equation-based approach to the analysis of real-life MMICS-application to microelectromechanical systems", *IEEE Trans. on Microwave Theory and Techniques*, Vol. 49 No. 12, pp. 2235-40.

Femlab (1997-2004), *Multiphysics modelling*, COMSOL, Inc., 1100 Glendon Avenue, 17th Floor Los Angeles, CA 90024, USA, available at: www.femlab.com

GetDP (2003), *A General Environment for the Treatment of Discrete Problems*, Department of Electrical Engineering (ELAP), Institut Montefiore, University of Liège, Sart Tilman Campus, available at: www.geuz.org/getdp, Belgium

Graglia, R.D. (1993), "On the numerical integration of the linear shape functions times the 3D Green's Function of its gradient on a plane triangle", *IEEE Trans. on Antennas and Propagation*, Vol. 41 No. 10, pp. 1448-55.

Nabors, K. and White, J. (1991), "Fastcap: a multipole accelerated 3D capacitance extraction program", *IEEE Transactions on Computer-Aided Design*, Vol. 10 No. 11, pp. 1447-59.

Pilkey, W.D. (2002), *Analysis and Design of Elastic Beams: Computational Methods*, Wiley, New York, NY.

Rao, S.M., Sarkar, T.K. and Harrington, R.F. (1984), "The electrostatic field of conducting bodies in multiple dielectric media", *IEEE Trans. on Microwave Theory and Techniques*, Vol. 32 No. 11, pp. 1441-8.

Rokhlin, V. (1983), "Rapid solution of integral equations of classical potential theory", *Journal of Computational Physics*, Vol. 60, pp. 187-207.

Saad, Y. and Schultz, M.H. (1986), "GMRES: a generalized minimal residual algorithm for solving nonsymmetric linear systems", *SIAM J. Sci. Comput.*, Vol. 7 No. 3, pp. 856-69.

Sabariego, R.V., Gyselinck, J., Dular, P., Geuzaine, C. and Legros, W. (2004), "Fast multipole acceleration of the hybrid finite element-boundary element analysis of 3D eddy current problems", *IEEE Transactions on Magnetics*, Vol. 40 No. 2, pp. 1278-1281.

Tilmans, H.A.C. (2002), "MEMS components for wireless communications (invited paper)", *Proc. EuroSensors XVI*, 15-18 September, Prague, Czech Republic, pp. 1-34 (CD-ROM only).